

The Analysis of Thermal Performance in an Airflow Window System Model

S.D. Park, Ph.D.

H.S. Suh, Ph.D.

S.H. Cho

ABSTRACT

The airflow window system originated in Scandinavia is a combination of energy-efficient fenestration and a solar energy collector. It consists of a double-glazed exterior window and a single-glazed interior window, with venetian blinds between these, as revealed previously in Finland and U.S.. The window provides excellent daylighting utilization as well as heating and cooling energy savings. It also provides thermal comfort and initial cost savings due to the capacity reduction of the utility equipment. This paper discusses the thermal performance of the airflow window system by theoretical analysis and a model experiment; basic experimental results of window system components and analytical results of the airflow window system model are provided. For the analysis of thermal properties of the airflow window system, a simulation program has been developed and the program will be continuously modified to make accurate energy analysis and estimation for different building applications.

INTRODUCTION

The insulation technology for the exterior envelope of a building has contributed to the building's energy savings until now. However, the counterplan for thermal performance improvement of the window that is the weakest point of the building has not been found yet. As one of the counterplans for thermal performance improvement of a window, research on the airflow window system began in the 1950s in Scandinavia. The first commercial building with an airflow window system was constructed in Helsinki in 1967.

The airflow window system is a combination of energy-efficient fenestration and a solar energy collector. It is composed of a double-glazed exterior window, a single-glazed interior window, and a venetian blind located in the air cavity between the external window pane and

the internal window pane. This system is comprised of three parts, as follows:

The first is called an exhaust air window. Room air is inflowd from the inlet at the top frame. The air flows downward through the window cavity and is exhausted to the outside of the room at the outlet of the bottom frame.

The second is called a supply air window. Outside air is inflowd from the inlet at the bottom frame. The air flows upward through the window cavity and is supplied to the inside of the room at the outlet of the top frame.

The third is called an air curtain window, a reference window. It has a colored aluminium frame and a thermal break called a venetian blind between the exterior window pane and the interior window pane. Room air is inflowd from the inlet at the bottom frame. The air flows upward through the window cavity and returns via a duct system to the central HVAC equipment.

Generally, the airflow window means the third class, the air curtain window. Since the energy crisis in 1973, many applications of the airflow window system to large-scale buildings showed the possibility of energy savings. Today, the airflow window system is adopted in about 100 buildings for thermal comfort in Scandinavia and central and northern Europe. Most buildings with the airflow window system are schools and hopperspitals. In the United States, the airflow window system has been applied to several residential buildings. The large-scale buildings with this system are found mostly in the West and the Midwest in the United States.

As a result of its application to many buildings, the amount of energy consumption in large-scale buildings with the airflow window system is 20% to 50% less than in buildings without it. The amount of energy collection of the airflow window system can be varied by the climate condition, the space between windows, the kind of venetian blinds, the size of the room air outlet and inlet, and the flow velocity in the air cavity. So far, the research on the above parameters' effect on thermal performance is not yet sufficient. Therefore, in this study, when the slat angle of the venetian blind is fixed at 90° horizontally, heat transfer and fluid flow in the airflow window system, with variations of inflowing airflow rate, will be analyzed by numerical analysis to predict the amount of energy collected by this system. The results predicted by numerical analysis will be compared with experimental results to check the accuracy of the numerical method. The data predicted by numerical analysis will be applied to apply to large-scale buildings with the airflow window system.

PHYSICAL MODEL

The schematic model of the airflow window system considered in the present study is shown

in Figure 1. The room air is inflowed through the inlet located at the bottom frame of this system. The room air being inflowed at a constant velocity is heated through heat transfer with the venetian blind while passing through the air cavity between a double-glazed exterior window and a single-glazed interior window. The air goes out through the outlet located at the top frame of this system. A rectangular duct exhausting the air from the outlet is settled on the roof, passing through a sunshade located at the exterior upper position of the experimental house. To change the velocity of inflowing air, the damper is installed in front of the blower located at the edge of the duct on the roof. The airflow window system is simplified to two dimensions since the window pane and venetian blind have sufficient length to neglect the Z-direction.

It is also assumed that the air outflowing from the outlet is fully developed flow and the top and bottom frame of the airflow window system are insulated. The airflow in the system is assumed laminar, incompressible, two-dimensional and forced convective. The present calculation is considered only when the angle of the venetian blind slat is fixed at 90° on horizontal. It is assumed that the heat conduction will dominate over the heat flow condition between the double-glazed exterior windows because the space between the double-glazed exterior windows is too narrow (0.24 in. [6mm]).

Actually the room air outlet faces the X-direction and is installed at the front direction of the exterior window. In this study, however, It is assumed that the outlet faces the Y-direction and the air is outflowed above this system for numerical analysis. The calculation domain of fluid flow and heat transfer for numerical analysis is shown in Figure 2 under the above assumptions. The specified numerical values of each variable applied for numerical analysis are listed in Table 1.

GOVERNING EQUATIONS AND BOUNDARY CONDITIONS

The governing equations of laminar, steady, incompressible, two nondimensional flow with constant properties are written as follows:

$$\frac{\partial u}{\partial x} + \frac{\partial v}{\partial y} = 0 \quad (1)$$

$$u \frac{\partial u}{\partial x} + v \frac{\partial u}{\partial y} = - \frac{\partial p^o}{\partial x} + C_1 \left(\frac{\partial^2 u}{\partial x^2} + \frac{\partial^2 u}{\partial y^2} \right) \quad (2)$$

$$u \frac{\partial v}{\partial x} + v \frac{\partial v}{\partial y} = - \frac{\partial p^o}{\partial y} + C_1 \left(\frac{\partial^2 v}{\partial x^2} + \frac{\partial^2 v}{\partial y^2} \right) \quad (3)$$

$$C_2 \left(u \frac{\partial \theta}{\partial x} + v \frac{\partial \theta}{\partial y} \right) = C_3 \left(\frac{\partial^2 \theta}{\partial x^2} + \frac{\partial^2 \theta}{\partial y^2} \right) + C_4 \quad (4)$$

The coefficients C_1, C_2, C_3, C_4 used in Equations 1 through 4 are as follows:

$$C_1 ; \frac{1}{Re}, \quad C_2 ; 1, \quad C_3 ; \frac{1}{Pe}, \quad C_4 ; 0 \text{ at air flow.}$$

$$C_1 ; \infty, \quad C_2 ; \frac{(\rho C_p)_s}{(\rho C_p)_f}, \quad C_3 ; \frac{1}{Pe} \cdot \frac{k_s}{k_f}, \quad C_4 ; \frac{Q_i}{Q_2} \cdot \frac{1}{w_i} \cdot \frac{1}{Pe}$$

at each window pane ($i = \text{each window pane}$) and

$$C_1 ; \infty, \quad C_2 ; \frac{(\rho C_p)_t}{(\rho C_p)_f}, \quad C_3 ; \frac{1}{Pe} \cdot \frac{K_t}{K_f}, \quad C_4 ; \frac{1}{t_1} \cdot \frac{1}{Pe}$$

at the venetian blind.

The dimensionless parameters in the above equations are defined as follows:

$$x = \frac{X}{H}, \quad y = \frac{Y}{H}, \quad t_1 = \frac{T_1}{H}, \quad w_1 = \frac{W_1}{H}, \quad w_2 = \frac{W_2}{H}, \quad w_3 = \frac{W_3}{H},$$

$$w_4 = \frac{W_4}{H}, \quad l = \frac{L}{H}, \quad h_1 = \frac{H_1}{H}, \quad h_t = \frac{H_t}{H}, \quad u = \frac{U}{U_o}, \quad v = \frac{V}{U_o},$$

$$Tr = \frac{Q_2 \cdot H}{k_f}, \quad \theta = \frac{T - T_o}{T_r}, \quad P^o = \frac{P}{(\rho U_o)^2}, \quad Re = \frac{U_o \cdot H}{\nu_f}, \quad Pe = Re \cdot Pr, \quad Pr = \frac{\nu_f}{\alpha_f}$$

The following boundary conditions for present calculation have been used:

$$u = v = 0, \quad \theta = \theta_o \quad \text{at } x = 0, \quad 0 \leq y \leq h$$

$$u = -1, \quad v = 0, \quad \theta = \theta_1 \quad \text{at } x = l, \quad 0 \leq y \leq h$$

$$u = v = 0, \quad \frac{\partial \theta}{\partial y} = 0 \quad \text{at } 0 < x < l, \quad y = 0$$

$$u = v = 0, \quad \frac{\partial \theta}{\partial y} = 0 \quad \text{at } 0 < x < l, \quad y = h_t$$

$$u = 0, \quad \frac{\partial v}{\partial y} = \frac{\partial \theta}{\partial y} = 0 \quad \text{at } 0 < x < h_1, \quad y = h_t$$

where θ_o, θ_1 are the dimensionless temperatures outside and inside the room and U_o is the

characteristic value of velocity.

Q1, Q2, Q3, and Q4 represent the heat flux of solar insolation absorbed by each window pane and venetian blind. They radiate heat flux when air passes through the air cavity between a double-glazed exterior window and a single-glazed interior window.

Q1, Q2, Q3, and Q4 are defined as follows:

$$Q1 = I_o \cdot A4 (1) \quad (5)$$

$$Q2 = I_o \cdot A4 (2) \quad (6)$$

$$Q3 = I_o \cdot A4 (3) \quad (7)$$

$$Q4 = I_o \cdot A4 (4) \quad (8)$$

Here, A4(1), A4(2), A4(3), and A4(4) are absorption ratios of the venetian blind and each window pane for solar insolation.

They are changed according to the incident angle of solar insolation and the venetian blind's slat angle. I_o represents solar insolation incident upon the airflow window system. When each window pane and venetian blind are composed of several layers (m layers), a method calculating total transmission, reflection, and each layer's absorption of solar insolation incident upon this system is derived as follows:

$$Tt(m) = Tt(m-1) Xr \quad (9)$$

$$Pt(m) = Tm + Tm Pt(m-1) Xr \quad (10)$$

$$At(m)n = At(m-1)n Xr \quad (n= 1,2... m-1) \quad (11)$$

$$At(m)m = Am + Am Pt(m-1) Xr \quad (12)$$

where $Xr = \frac{Tm}{1 - Pm Pt(m-1)}$

$$Tt(1) = T1, \quad Pt(1) = P1, \quad At(1)1 = 1 - T1 - P1$$

Here, $Tt(m)$ and $Pt(m)$ are the total transmission and reflection to m layers. $At(m)n$ is the n 'th layer's absorption when total layers are composed of m layers and Tm is the transmission of the m 'th layer. By using the above calculation method, the calculation results of the absorption of the venetian blinds and each window pane are:

$$A4(1) = 0.0, \quad A4(2) = 0.68, \quad A4(3) = 0.07, \quad A4(4) = 0.09$$

Here 4 means four layers composed of three window panes and a venetian blind; (1) means the pane of single glazing, (2) means the venetian blind, (3) means the internal pane of double glazing, and (4) means the external pane of double glazing.

The value of thermal properties (absorption, reflection, transmission) of the window

pane (0.2 in. [5mm]) and venetian blind slat (painted black) used to calculate the total transmission, reflection, and each layer's absorption was adopted by 0.071, 0.077, and 0.852 at each window pane and 0.956, 0.044, and 0.0 at the venetian blind slat where thermal properties of the window pane and venetian blind slat were the value measured by a solar spectrum reflection meter.

The subscript f at each variable represents the property of 300K air (pr: 0.7) whose thermal conductivity is $K_f = 0.0152 \text{ Btu/h.ft}^\circ\text{F}$ ($0.0246 \text{ W/m}^\circ\text{C}$).

The conductivities of the glass and venetian blind are assumed to be:

$$K_g = 0.45 \text{ Btu/h. ft}^\circ\text{F} (0.78 \text{ W/m}^\circ\text{C}), \quad K_t = 117 \text{ Btu/h.ft}^\circ\text{F} (204 \text{ W/m}^\circ\text{C})$$

The value of solar insolation on the south-facing vertical plane (I_o) was 150 Btu/h.ft^2 (504 W/m^2) measured by a spectral pyranometer from 10 a.m. to 11 a.m. on February 22, 1989. in Dae Jeon, Korea. Measured mean temperature outside and inside the room at the above time were 10°C and 23°C , respectively. The window size of the airflow window system is 1.3 by 2.2 m.

SOLUTION PROCEDURE

Equations 1 through 4 are discretized by the method of control volume formulation. The final discretization equations have a generalized form on a grid point p.

$$a_p \phi_p = \sum_{nb} a_{nb} \phi_{nb} + b \quad (13)$$

where ϕ_p denotes u, v , and θ and the subscript nb denotes the neighbor grid points of p.

The summation is to be taken over all neighbors. In the present study, there are four neighbors. The discretization equations are solved by a finite difference calculation procedure called SIMPLE (Semi Implicit Method for Pressure Linked Equation). A 25 by 70 grid was employed with a denser nodal point spacing near the walls and the window panes. Using a PC, about 1500 to 2000 iterations were needed to get a convergent solution. The criterion of convergency was taken when the values of each variable didn't vary within four digits during 10 continuous iterations.

MEASUREMENT OUTLINE

To check the accuracy of the computer simulation program developed in this study, the

measurement of the air velocities and temperatures was done on an airflow window system rebuilt from an existing window of an experimental house. The experimental house is a one-story single-family detached house. The airflow window system is installed in a room on the south side. As seen in Figure 3, the floor area of this house is 911 ft^2 (85.70 m^2) with a radiator heating system. The room with the airflow window system is kept at a constant temperature by an automatic controller. The duct exhausting air from the outlet is settled on the roof, passing through a sunshade at the exterior upper position of the house. A damper is installed in front of the blower at the edge of the duct on the roof to change the velocity of inflowing air. During the period of experiment from February 22, to March 9, 1989, the weather was partly cloudy. As the computer simulation program developed for this study was done under the assumption of ideal conditions (sunny and the outside temperature was constant), the experimental results of February 22, 1989 whose weather was similar to the ideal condition assumed by numerical analysis, were adopted for comparison with the results of numerical analysis.

Figure 4 is a photograph of the airflow window system installed at the experimental house.

SOLAR INSOLATION MEASUREMENT

The instrument used to measure solar insolation incident upon the airflow window system was a spectral pyranometer. The measured data were recorded by mean value every hour.

TEMPERATURE MEASUREMENT

Temperature measurement was done automatically and thermocouples settled in measuring points were connected to a data logger. The thermocouples-copper-constantans-were specially covered by aluminium foil to break direct solar insolation.

FLOW VELOCITY MEASUREMENT

Anemomasters were chosen to measure flow velocity at the inlet and outlet of the system. Data measured every minute were used by mean value.

Figure 5 presents temperature and velocity measuring points. There were 32 total points of temperature measurement and 2 points for flow velocity measurement.

COMPARISON OF NUMERICAL RESULTS AND EXPERIMENTAL RESULTS

To check the accuracy of the numerical analysis results when the angle of the venetian blind slat was fixed at 90° on horizontal, the experimental results of horizontal temperature distribution at $Y = 0.82, 1.64, \text{ and } 2.4 \text{ ft}$ ($0.25, 0.5, \text{ and } 0.75 \text{ m}$) when the air velocity at the inlet was 1.64 ft/s (0.5 m/s) was compared to the numerical analysis results. The solar insolation measured by the spectral pyranometer at the south side of the experimental house in Dae Jeon was 159 Btu/h.ft^2 (504 W/m^2). Six measuring points were fixed to measure the room's inside and outside temperature. The mean values of the measured temperatures were 10°C and 23°C .

Figure 6 shows the horizontal temperature distribution at the vertical height $Y = 0.82, 1.64, \text{ and } 2.4 \text{ ft}$ ($0.25, 0.5, \text{ and } 0.75 \text{ m}$) when the air velocity inflowing at the air inlet is 1.64 ft/s (0.5 m/s). Generally, it shows the maximum temperature is found at venetian blind $X = 0.299 \text{ ft}$ (0.091 m) and temperature values at the left-side flow field of the venetian blind are higher than the right-side flow field. The temperature distribution by numerical analysis on a horizontal line in the air-flow window system is increased when the vertical height is higher but the temperature distribution by experimental result is not always changed. In general, the temperature distribution's trend on a horizontal line by numerical analysis and experimental measurement is uniform. But the temperature distribution by numerical analysis is a little higher. This is because the temperature by experimental measurement is decreased, owing to a sunshade on the top frame of the airflow window system.

DISCUSSION

Experiment and numerical analyses for temperature distribution in an airflow window system have been performed when the angle of a venetian blind slat is fixed at 90° on horizontal.

The size of a slat's cross area is $0.98 \text{ by } 0.14 \text{ in.}$ ($25 \times 0.1 \text{ mm}$) and the venetian blind is composed of 55 slats. The space between a double-glazed exterior window and a single-glazed interior window is 0.49 ft (0.15 m) deep and a black venetian blind is installed in the middle of the space. The air temperature inflowing in the airflow window system is 23°C (measured value) and the Prandtl number is 0.7. The height of the air inlet at the bottom frame is 0.39 in. (10 mm). The height of the air outlet on the top frame is 0.78 in. (20 mm).

This study is to find how the variation of the air flow rate inflowing into the airflow window system affects velocity distribution, temperature distribution, and energy collected. The inflowing velocities at the air inlet are 0.656 ft/s (0.2 m/s), 1.64 ft/s (0.5 m/s), 3.28 ft/s (1.0 m/s), 6.65 ft/s (2.0 m/s), and 8.33 ft/s (2.5 m/s). The Reynolds numbers of these velocities are 118, 297, 584, 1188, and 1485, respectively.

STREAMLINE DISTRIBUTION

Figure 7 shows dimensionless streamline distribution when the variations of the Reynolds number are 118, 297, 584, 1188, and 1485. The values of dimensionless stream function $\varphi = \int u dy$ are -0.15, -0.3, -0.45, -0.6, -0.75, and -0.9. Negative (-) represents the direction of airflow in which air inflowing from the inlet at the bottom frame of the airflow window system flows out to the outlet at the top frame. A clockwise recirculation is found at the lower flow field of the venetian blind's left side at all Reynolds numbers considered in this study. The size of recirculation expands as the Reynolds number increase, so that it expands to the upper area of the venetian blind from (Re = 1188).

Maximum stream function ("X") exists in the middle of clockwise recirculation. The location of maximum stream function appears at the lower area of the air cavity, although the Reynolds number increases. Since the Reynolds number is higher than 297, most stream function appears in the left-side flow field of the venetian blind. It means that most of the airflow passes through the venetian blind's left-side flow field.

DIMENSIONLESS TEMPERATURE DISTRIBUTIONS

Figure 8 shows isothermal lines divided into six parts from maximum to minimum temperature when the Reynolds numbers are 118, 297, 584, 1188, and 1485. The distribution of isothermal lines is denser at the left-side flow field than at the right-side flow field when the Reynolds number is more than 297.

It means that the heat flux generated at the venetian blind is emitted more to the left-side flow field than to the right-side flow field. This is because the temperatures of single glazing at the right side of the venetian blind are higher than the temperatures of double glazing at the left side and almost all the air flow passes through the blind's left-side flow field. For all Reynolds numbers chosen in this study, the isothermal distribution is denser in the

lower flow field near the air inlet than in the upper. It means that heat flux radiating from the venetian blind to the air decreases more at the upper flow field than at the lower flow field between a double glazing and a single glazing. This is because the flowing air moves to the upper flow field after the temperature of inflowing air increases through heat transfer with the venetian blind at the lower flow field near the inlet of the inflowing air.

TEMPERATURES AT THE OUTLET AND ENERGY COLLECTED BY THE SYSTEM

To get the energy collected by the system on the variations of the airflow rate inflowing to the airflow window system, the formula is:

$$q = \int_{T_i}^{T_o} \rho C_p \dot{m} dT$$

where T_i is the temperature inflowing through the air inlet and T_o is the bulk temperature at the outlet.

The definition of bulk temperature at the outlet is:

$$T_o = \frac{\int T dx}{\int dx}$$

Figure 9 shows bulk temperature at the outlet and energy (q) collected by this system on the variations of inflowing airflow rate (variations of Reynolds number). When the Reynolds number is 118, the highest dimensionless temperature is 0.11; it is 13°C in dimensional temperature. Dimensionless temperature drops rapidly as the Reynolds number increases, so it drops down to 0.009 when the Reynolds number is 1485. Energy (q) collected by this system increases until the Reynolds number increases to 584. But at more than 584, energy (q) shows a constant value. Therefore, the proper airflow rate for the airflow window system adopted in this study is $\dot{m} = 4.237 \text{ ft}^3/\text{min}$ ($0.12 \text{ m}^3/\text{min}$), when the Reynolds number is 584.

CONCLUSION

In this study, when the venetian blind's slat angle is fixed at 90° on horizontal, heat transfer and fluid flow in the airflow window system on the variations of inflowing airflow

rate were analyzed by numerical analysis to predict the fluid temperature at the outlet and the energy collected by this system. Absorption and reflection of a slat and solar insolation per hour were measured for basic input data for numerical analysis. To check the accuracy of numerical analysis, the comparison was done between experimental results at an experimental house and results of numerical analysis and it was a uniform trend. Numerical analysis for heat transfer and fluid flow in the airflow window system was done by the SIMPLE (Semi Implicit Method for Pressure Linked Equation) procedure. The effects of the variation of inflowing airflow rate on fluid flow and temperature distribution in the airflow window system are as follows:

- 1) As Reynolds number goes higher than 297, almost all airflow passes through the leftside flow field of the venetian blind.
- 2) A clockwise recirculation is found at the lower flow field of the venetian blind's left side at all Reynolds numbers considered in this study. The size of recirculation expands at the Reynolds number increases.
- 3) Energy (q) collected by the airflow window system model considered in this study shows a constant value when the Reynolds number is more than 584. Therefore, the proper airflow rate for this system is $\dot{m} = 4.237 \text{ ft}^3/\text{min}$ ($0.12 \text{ m}^3/\text{min}$) when the Reynolds number is 584.

REFERENCES

- Muller, H. 1984. "Exhaust air ventilated windows in office buildings." ASHRAE Transactions. Vol. 90, pp. 932-947.
- Parmelee, G.V., and Aubele, W.W. 1952. "The shading of sunlit glass." ASHVE Transactions, pp. 377- 398.
- Patankar, S.V. Numerical heat transfer and fluid flow. New York: McGraw-Hill Book Company.
- Punntila, J.A., and Enbom, S.A. 1983. "Heat transfer calculations of different types of window systems." The Fourth International Symposium on the Use of Computers for Environmental Engineering related to Buildings, pp. 152-155.
- Ripatti, H. 1984. "Airflow window system-making fenestration the solution rather than the problem in energy use." ASHRAE Transactions. Vol. 90, Part 1.
- Siegel, R., and Howell, J.R. Thermal radiation heat transfer. New York: McGraw-Hill Book Company.

TABLE 1

Specification of Each Parameter Used in the Airflow Window System Model

Parameters	H_1	H_2	Ht	L	S_1
Scale ft (m)	0.03(0.01)	0.056(0.02)	4.26(1.3)	0.56(0.17)	0.48(0.15)
Parameters	W_1	W_2	W_3	W_4	T_1
Scale ft (m)	0.016(0.005)	0.016(0.005)	0.019(0.006)	0.016(0.005)	0.003(0.001)

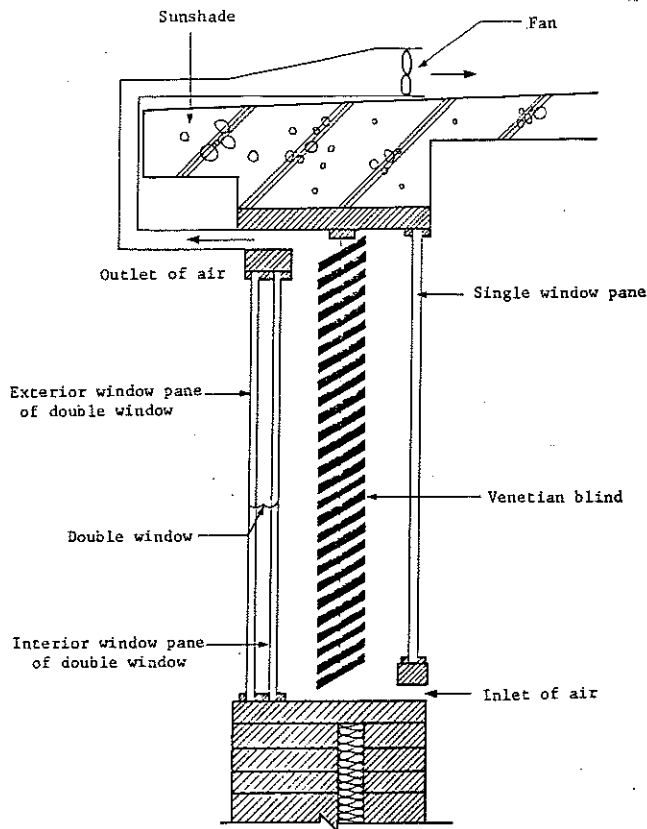


Figure 1. Schematic diagram of air-flow window system

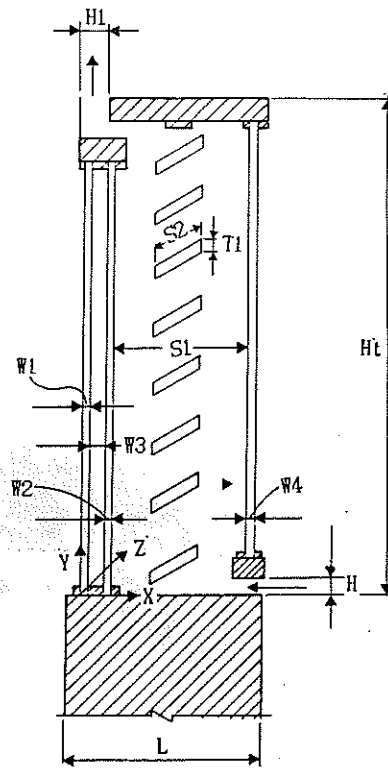


Figure 2. Specification of calculation domain

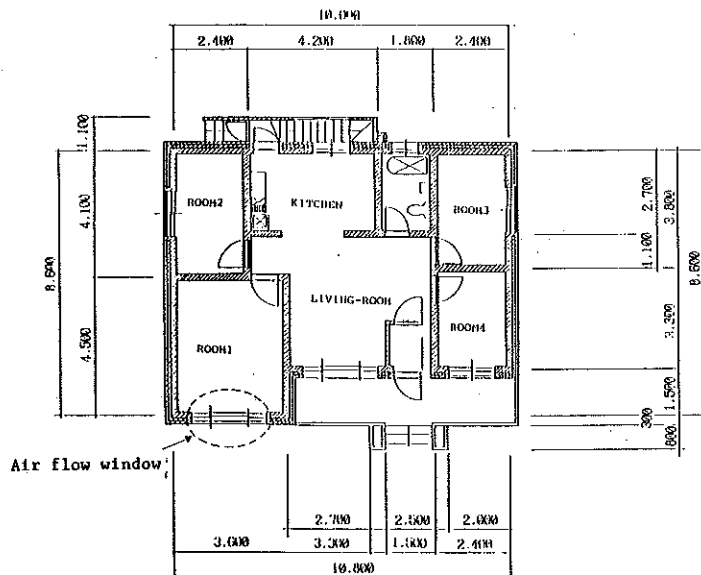


Figure 3. Plane figure of experimental house

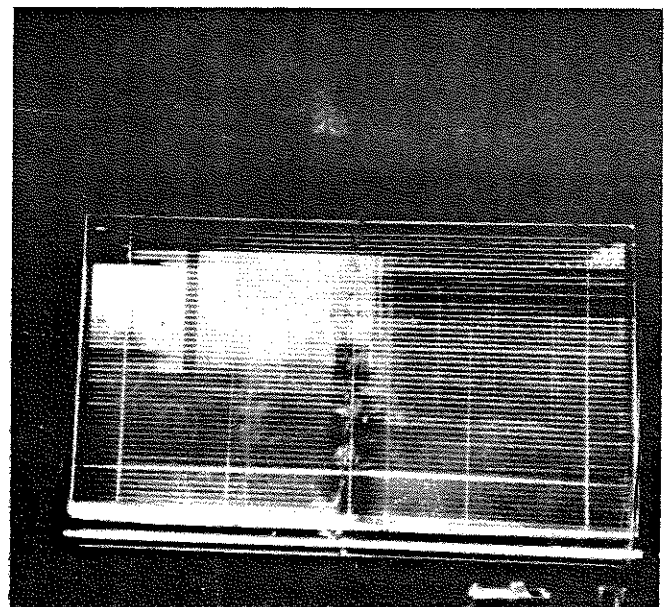


Figure 4. Photograph of airflow window system installed in experimental house

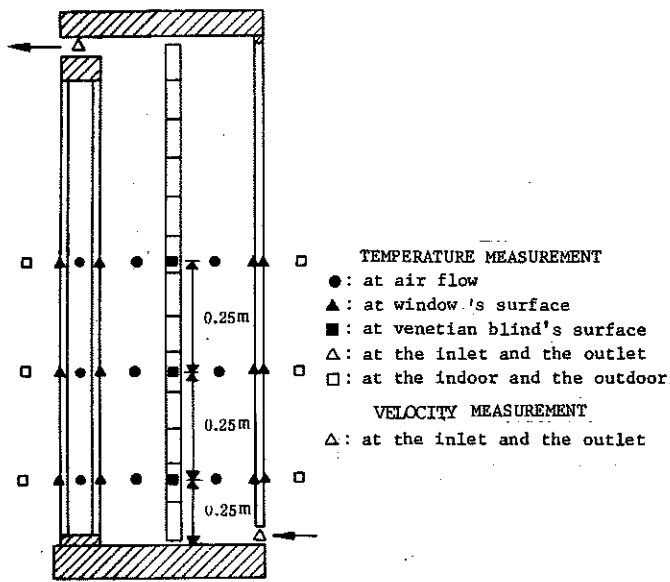


Figure 5. Measuring points of temperature and velocity

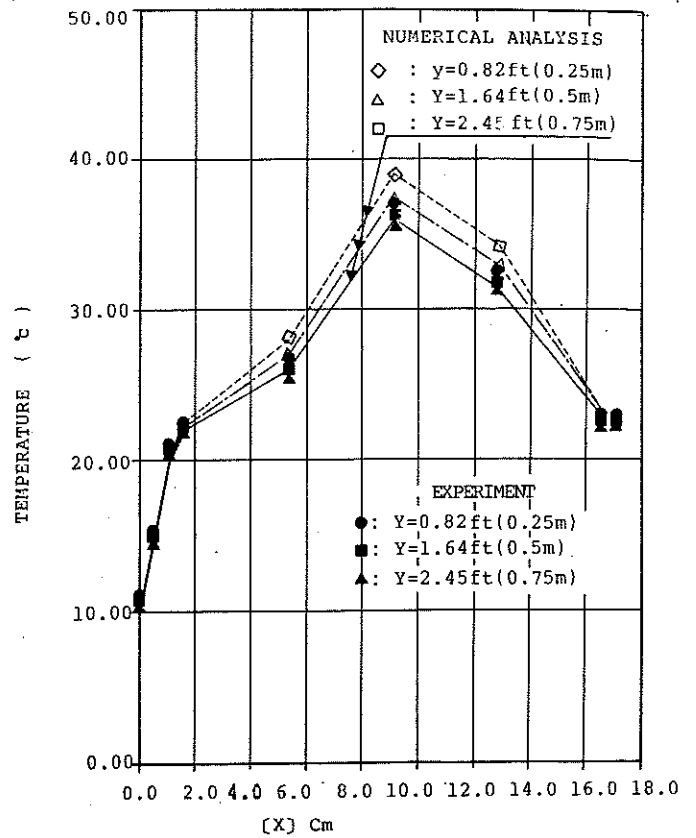


Figure 6. Comparison of temperature distribution by numerical analysis and experiment at $Y=0.82, 1.61, 2.1$ ft. (0.25, 0.5, 0.7m)

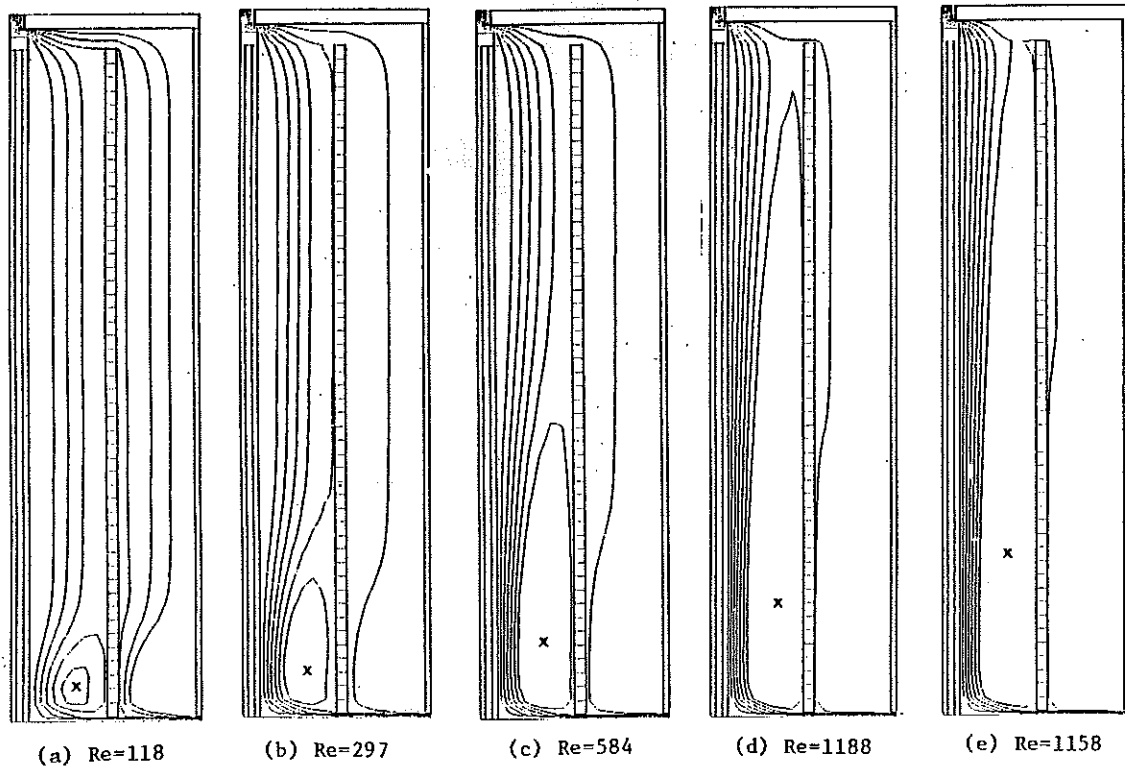


Figure 7. Streamline distribution in airflow window system

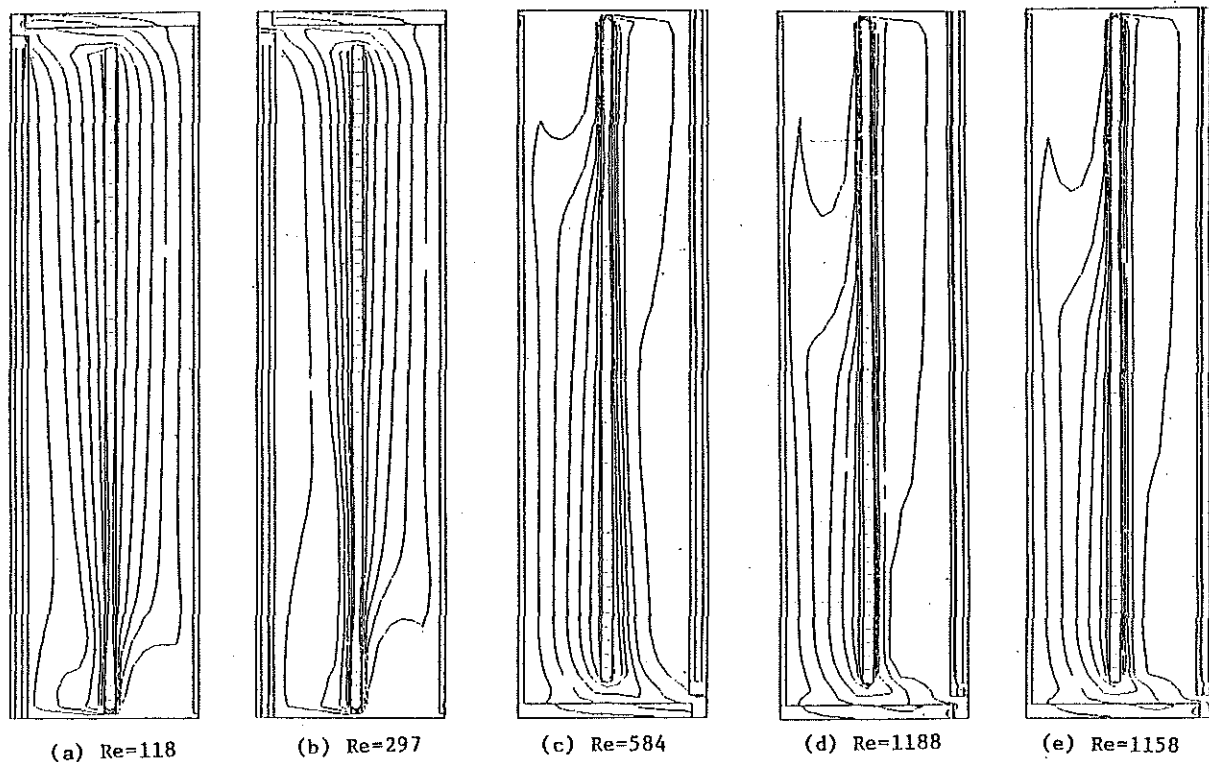


Figure 8. Distribution of isotherms in airflow window system

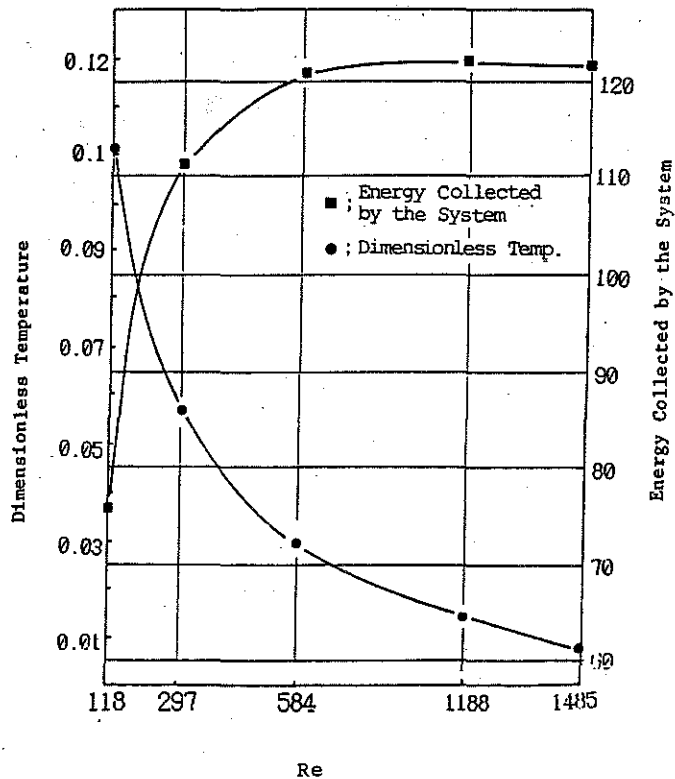


Figure 9. Heat capacity and dimensionless temperature at the outlet